Seismic imaging of marine crustal structure with high resolution and uncertainty quantification and utilization of the structural information

Project Representative
Ryoichiro Agata, Subduction Dynamics Research Center, Research Institute for Marine Geodynamics, Japan Agency for Marine-Earth Science and Technology

Authors
Kota Mukumoto*[1], Yanfang Qin*[2], Gou Fujie*[2], Ryoichiro Agata*[2] and Jun Su*[2]

*[1] Barcelona Center for Subsurface Imaging, Institut de Ciencies del Mar, The Spanish National Research Council

*[2] Subduction Dynamics Research Center, Research Institute for Marine Geodynamics, Japan Agency for Marine-Earth Science and Technology

Keywords : Nankai Trough, accretionary prism, full waveform inversion, subduction zone, seismic imaging, physics-informed neural network

1. Development of high-performance wave simulation software serving as a foundation for high-precision and high-resolution seismic imaging

Conventional seismic imaging has visualized subsurface structures by extracting partial information, such as first arrival times and dispersion characteristics, from observed waveform data. However, with recent dramatic improvements in computational performance, methods such as Full Waveform Inversion (FWI) and Reverse Time Migration (RTM), which maximize the utility of observed data based on full wavefield calculations, have become widely adopted. These methods enable the visualization of subsurface structures with higher precision and resolution compared to conventional techniques, becoming game-changers in the fields of resource exploration and seismology.

Since full wavefield calculations require large-scale numerical computations, simulation software capable of high-speed and high-efficiency execution is indispensable. In this study, we developed SEM-SWS (Spectral Element-based Seismic Wave Simulator), a seismic wave simulation software capable of computing on both CPUs and GPUs. Based on the spectral element method (a type of high-order finite element method), SEM-SWS solves viscoelastic acoustic and elastic wave equations.

By leveraging the ecosystem of the MFEM (Modular Finite Element Methods) library, this software enables computations on both CPUs and GPUs (CUDA and HIP) from a single codebase. Designing the software to rely on MFEM for GPU support has improved code maintainability and future scalability.

For performance evaluation, strong and weak scaling tests were conducted using the Earth Simulator. GPU-Aware MPI was utilized for GPU parallel computations. Fig. 1 shows the results of the scalability tests on CPUs. In both strong and weak scaling, scores exceeded 100%, confirming high parallel efficiency. Fig. 2 presents the results of the scalability tests on GPUs. In the strong scaling test, a parallel efficiency of 86.5% was achieved with a configuration of 4 nodes (32 GPUs). In the weak scaling test, while efficiency was 100% for parallel computation on a single node, it was 92.1% on two nodes. Despite overhead from inter-node communication, high overall parallel performance was achieved.

Fig. 3 illustrates the performance comparison between GPUs and CPUs using the strong scaling test results. We evaluated the computational performance of one GPU node relative to the equivalent number of CPU nodes on the Earth Simulator. For a problem size of 256×256×80 elements (approximately 340 million mesh points), the computational performance of SEM-SWS on one GPU node was found to be equivalent to that of 32 CPU nodes.

Currently, SEM-SWS supports forward modeling of seismic wavefields. However, we plan to implement FWI and RTM in the coming fiscal year and beyond. Furthermore, since marine seismic exploration requires accounting for the interaction between solids and liquids, we also plan to implement forward modeling capabilities that incorporate solid-fluid coupling.

2. Full Waveform Inversion (FWI) of the region near the 2024 Noto Earthquake Rupture Zone

During this year, we used the ES facility extensively for a research project focused on the rupture zone of the 2024 Noto earthquake. The main objective of this study is to reconstruct the subsurface seismic velocity structure using ocean-bottom seismometer (OBS) data through waveform tomography. This approach requires large-scale numerical simulations and iterative inversions, involving repeated forward and adjoint wavefield calculations, which are computationally intensive and demand significant parallel computing resources. Preliminary results reveal low-velocity zones beneath the rupture area, potentially related to fluid-rich regions, providing new insights into the earthquake rupture mechanism (Fig. 4).

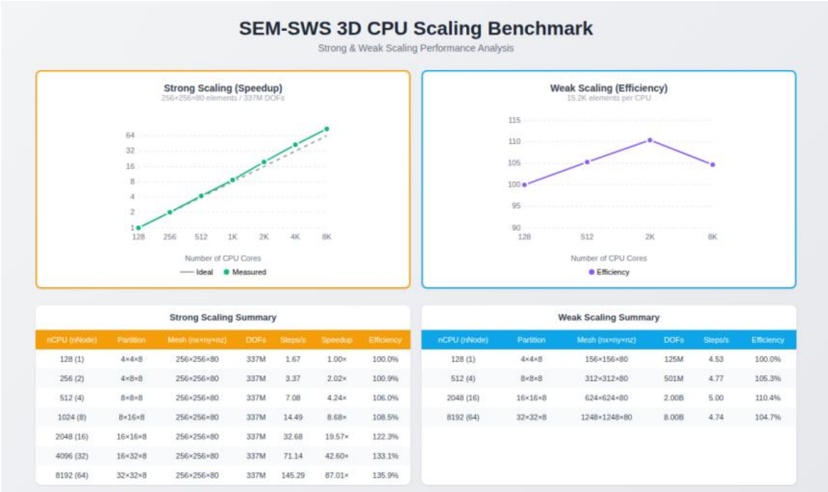

Strong Scaling Summary

nCPU (nNode)	Partition	Mesh (nx×ny×nz)	DOFs	Steps/s	Speedup	Efficiency
128 (1)	4×4×8	256×256×80	337M	1.67	1.00×	100.0%
256 (2)	4×8×8	256×256×80	337M	3.37	2.02×	100.9%
512 (4)	8×8×8	256×256×80	337M	7.08	4.24×	106.0%
1024 (8)	8×16×8	256×256×80	337M	14.49	8.68×	108.5%
2048 (16)	16×16×8	256×256×80	337M	32.68	19.57×	122.3%
4096 (32)	16×32×8	256×256×80	337M	71.14	42.60×	133.1%
8192 (64)	32×32×8	256×256×80	337M	145.29	87.01×	135.9%

Weak Scaling Summary

nCPU (nNode)	Partition	Mesh (nx×ny×nz)	DOFs	Steps/s	Efficiency
128 (1)	4×4×8	156×156×80	125M	4.53	100.0%
512 (4)	8×8×8	312×312×80	501M	4.77	105.3%
2048 (16)	16×16×8	624×624×80	2.00B	5.00	110.4%
8192 (64)	32×32×8	1248×1248×80	8.00B	4.74	104.7%

Fig.1 CPU scalability test results. The top two panels illustrate the speedup achieved in strong scaling tests and the parallel efficiency observed in weak scaling tests. The bottom two tables present details for each test, including partitions in the x, y, and z directions, the number of elements (mesh), degrees of freedom (DOFs), computational speed (Steps/s, SpeedUp), and parallel efficiency.

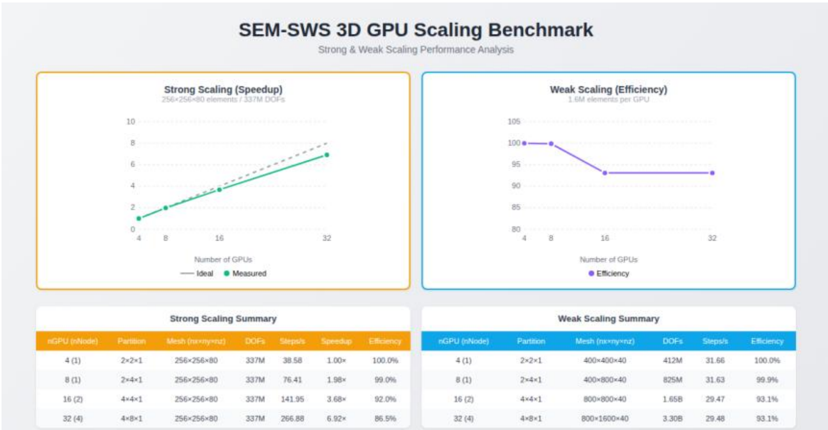

Strong Scaling Summary

nGPU (nNode)	Partition	Mesh (nx×ny×nz)	DOFs	Steps/s	Speedup	Efficiency
4 (1)	2×2×1	256×256×80	337M	38.58	1.00×	100.0%
8 (1)	2×4×1	256×256×80	337M	76.41	1.98×	99.0%
16 (2)	4×4×1	256×256×80	337M	141.95	3.68×	92.0%
32 (4)	4×8×1	256×256×80	337M	266.88	6.92×	86.5%

Weak Scaling Summary

nGPU (nNode)	Partition	Mesh (nx×ny×nz)	DOFs	Steps/s	Efficiency
4 (1)	2×2×1	400×400×40	412M	31.66	100.0%
8 (1)	2×4×1	400×800×40	825M	31.63	99.9%
16 (2)	4×4×1	800×800×40	1.65B	29.47	93.1%
32 (4)	4×8×1	800×1600×40	3.30B	29.48	93.1%

Fig. 2 GPU scalability test results. The top two panels illustrate the speedup achieved in strong scaling tests and the parallel efficiency observed in weak scaling tests. The bottom two tables present details for each test, including partitions in the x, y, and z directions, the number of elements (mesh), degrees of freedom (DOFs), computational speed (Steps/s, SpeedUp), and parallel efficiency.

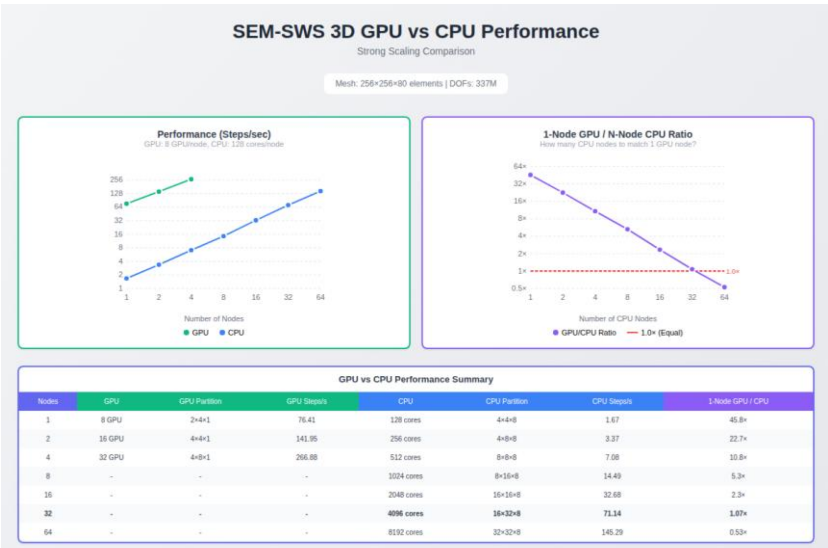

GPU vs CPU Performance Summary

Nodes	GPU	GPU Partition	GPU Steps/s	CPU	CPU Partition	CPU Steps/s	1-Node GPU / CPU
1	8 GPU	2×4×1	76.41	128 cores	4×4×8	1.67	45.8×
2	16 GPU	4×4×1	141.95	256 cores	4×8×8	3.37	22.7×
4	32 GPU	4×8×1	266.88	512 cores	8×8×8	7.08	10.8×
8	-	-	-	1024 cores	8×16×8	14.49	5.3×
16	-	-	-	2048 cores	16×16×8	32.68	2.3×
32	**-**	**-**	**-**	**4096 cores**	**16×32×8**	**71.14**	**1.07×**
64	-	-	-	8192 cores	32×32×8	145.29	0.53×

Fig. 3 Performance comparison between GPUs and CPUs based on strong scaling test results.

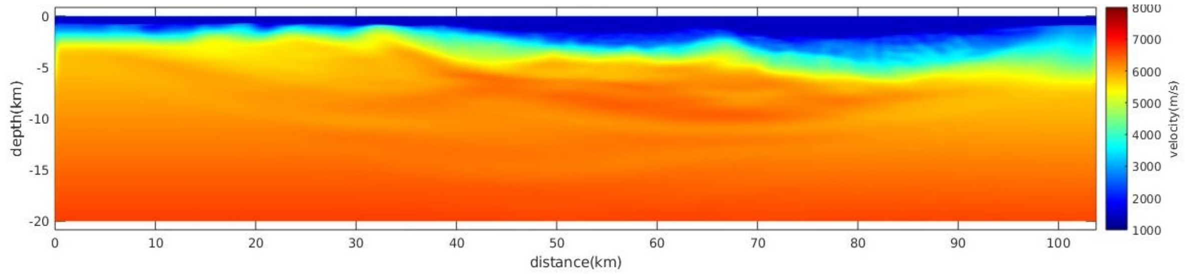

Fig.4 A preliminary result of FWI for P-wave velocity in the region near the 2024 Noto Earthquake Rupture Zone

3. Optimization of OBS Spacing for FWI in Subduction Zones

Plate subduction zones host a variety of geodynamic processes, including megathrust earthquakes. Subsurface structure is fundamental for understanding these processes. Marine controlled-source seismic surveys are the most effective approaches for revealing detailed subsurface structures in this region.

These surveys are generally classified into two types: wide-angle seismic surveys using ocean-bottom seismometers (OBSs), and multi-channel seismic reflection (MCS) surveys using long streamer cables equipped with dense hydrophone arrays. OBS data are mainly used to estimate seismic velocity structures from long-offset refraction traveltimes although the resulting models have low spatial resolution.

In contrast, MCS data are well suited for imaging seismic reflectors and structural interfaces, such as sediment-crust boundaries and plate boundaries. Appropriate velocity structure is required to convert reflection two-way travel times into depth. However, MCS data alone can constrain velocities only to depths comparable to the streamer length. In subduction zones, the plate interface—lies at depths of approximately 5-30 km in the Nankai Trough and 10-50 km in the Japan Trench, significantly deeper than our streamer length (6 km). Therefore, to discuss detailed geometry of the plate interface, we need to provide more reliable velocity information for depth-conversion.

Full-waveform inversion (FWI) of OBS data, exploiting waveform information beyond traveltime alone, can substantially improve spatial resolution. We confirmed that the geometry of the plate interface is significantly improved by combining MCS reflection data with velocity models derived from OBS FWI, based on the actual data set obtained in Nankai Trough off Muroto Cape.

Effective application of FWI requires denser OBS spacing than that typically used for traveltime-based analyses. Increasing the number of OBSs, however, directly increases survey cost in terms of both time and budget. It is therefore necessary to identify an optimal OBS spacing that balances imaging performance with economic feasibility. To this end, we applied FWI to the dataset of 1 km OBS spacing while gradually reducing the number of OBSs (increasing the OBS spacing) to investigate the effects of decimating OBSs. Our results indicate that an OBS spacing of 2 km provides an effective compromise between spatial resolution and survey cost for the subduction zone structure studies.

4. Bayesian 3D first-arrival travel time tomography using physics-informed neural networks

First-arrival travel time tomography (FAT) is essential for subsurface velocity modeling, yet quantifying uncertainty remains a challenge. While traditional Bayesian approaches often rely on grid-based discretization, we previously developed a mesh-free Bayesian framework using Physics-Informed Neural Networks (PINN) [1]. In this study, we extend this framework to three-dimensional (3D) space. We demonstrate the effectiveness of this novel 3D approach through numerical experiments that assume the combined use of active source seismic data and natural earthquake data.

To extend the method to three-dimensional problems, we implemented sparsification and acceleration techniques for constructing the covariance matrix and solving linear systems, which are required to calculate the prior probability density of the velocity structure. This work was carried out with the assistance of the "Juten" (重点) support provided by the Earth Simulator support team.

We employ a synthetic 3D velocity model characterized by a depth-dependent background overlaid with sinusoidal anomalies of varying wavelengths. The observation geometry simulates a combination of active source survey lines and passive seismic events (Fig. 5). Although not detailed here, we incorporate a method to account for significant uncertainty in passive source locations. Using our proposed approach, the estimated mean velocity structures in the shallow regions agree well with the true velocity structure, demonstrating the success of our 3D extension (Fig. 6). Although the deeper regions are slightly affected by bias due to source mislocation, we confirmed that these artifacts are significantly reduced compared to previous methods.

We are currently applying this method to actual field data from the Nankai Trough to estimate its 3D structure.

5. Establishment of Machine Learning Noise Reduction Method

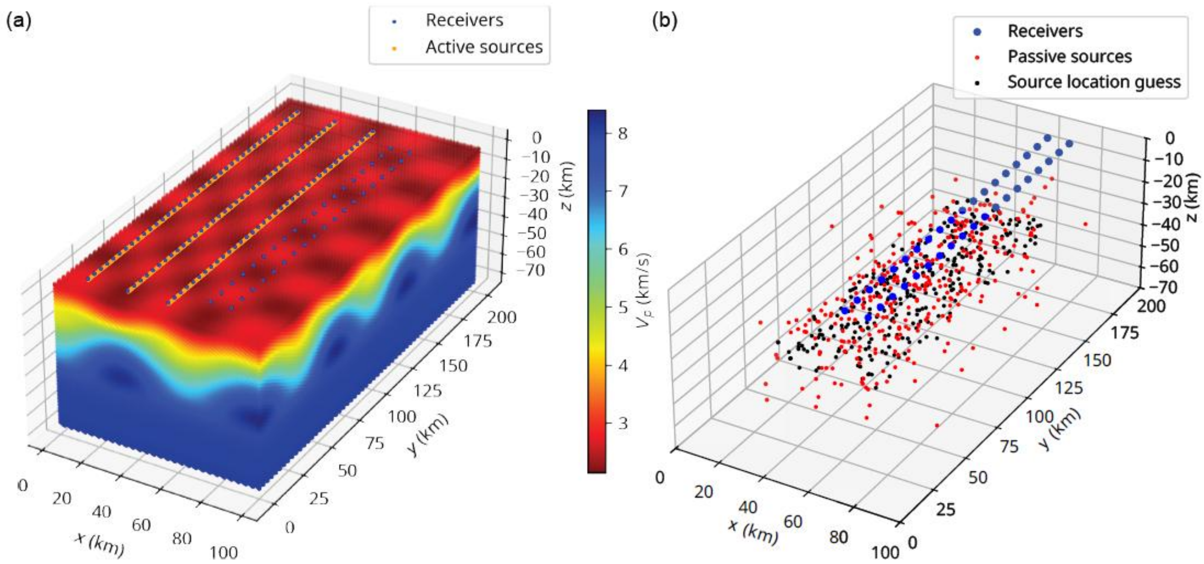

Fig.5 (a) Synthetic velocity structure and active source/receiver positions. (b) Passive natural earthquake source and receiver positions.

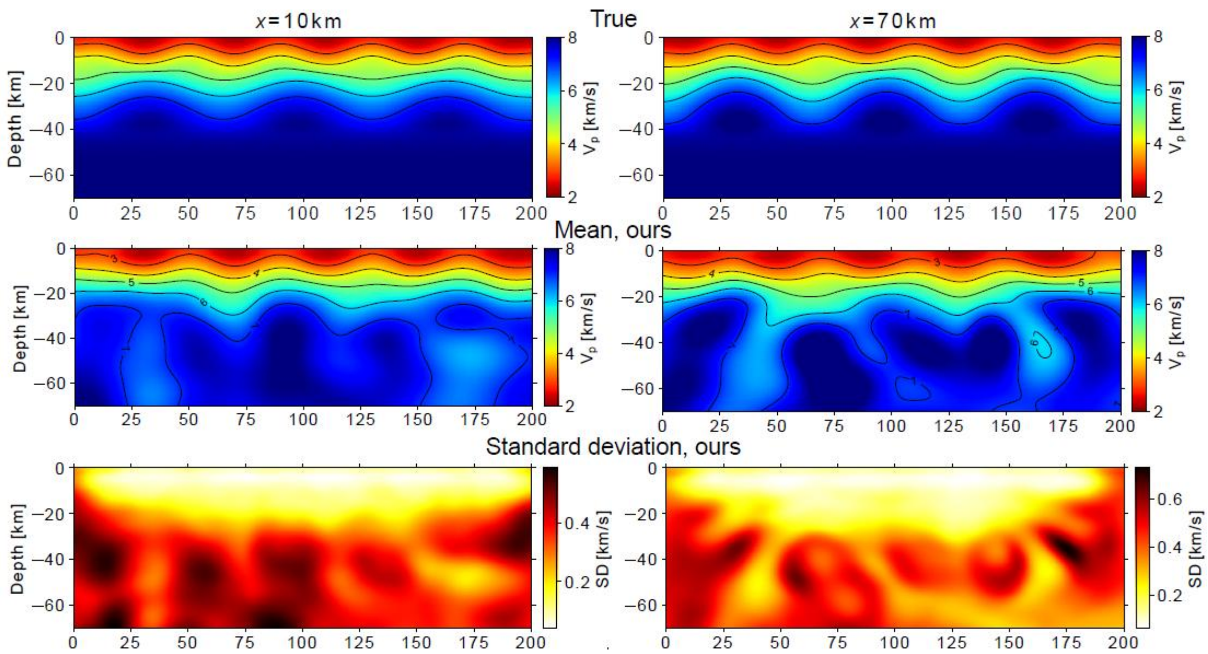

Fig.6 Comparison of the true model, the estimated mean and standard deviation at two cross sections.

During the wide-angle seismic surveys, controlled seismic sources, typically the tuned air-gun arrays, are fired to generate impulsive seismic signals, which are then recorded by pre-deployed OBS as they propagate beneath the seafloor. In order to obtain a reliable subsurface structure, noise reduction is a crucial preprocessing step to remove the unwanted random or systematic waveform components introduced during the source generation and wave measurement.

Environmental noise depends on the time and the location of an external source, or is even random, making stacking methods effective to reduce the noise. Different environmental noise sources have different characteristic times and space ranges. Diversity stacking is a widely used technique to remove this time-varying noise, but it requires repeating the firing of the source, substantially increasing acquisition costs in marine seismic surveys.

On the other hand, for long-offset OBS stations, water waves from previous shots have high amplitudes and can also overlap with primary refraction phases of the subsequent shot, contaminating the data, when the airgun source is fired at a short interval, such as in MCS surveys. This kind of noise is hard to

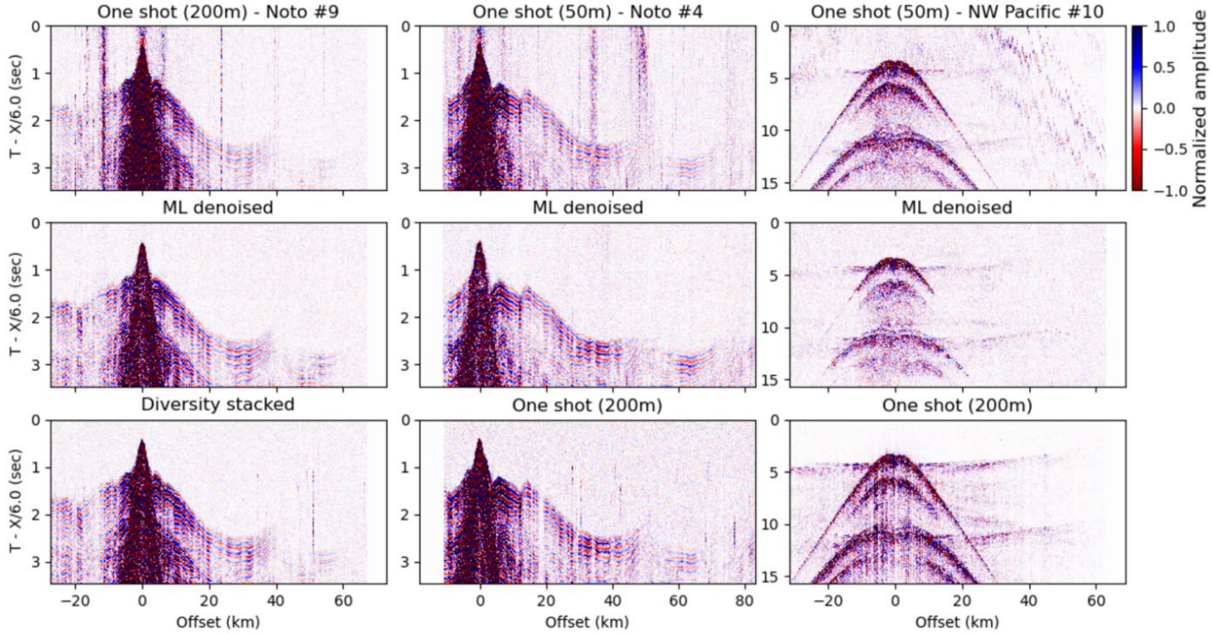

Fig. 7 The comparison between pre-stacked (top), denoised (middle), and reference data obtained with a higher data acquisition cost (bottom).

remove and makes the phase picking difficult due to the large amplitude contrast between the signal and the noise.

This study seeks to take advantage of machine learning methods to address these limitations of conventional methods, which suffer from the high survey cost from stacking repeated surveys and from being unable to use short-offset MCS data for wide-angle surveys. We present an automated approach using a denoising diffusion probabilistic model (DDPM), a generative machine learning technique proven successful in image processing. Following the approach by Durall et al. (2023) [2], we trained the DDPM on a field dataset with high signal-to-noise ratio (S/N) waveforms via stacking for the first time.

A survey fired five times with a 200-m interval near the Noto Peninsula is used to train our model, and the outcome denoising method successfully suppresses the noise and achieves a high S/N similar to the diversity stacking results by only using pre-stacked record sections (Fig. 7). The denoised record section achieves improvements in first-arrival picking and cross-correlation alignment, which may help to obtain a more reliable structure with first-arrival tomography and FWI. Additionally, the results applying to the test data with a 50-m shot interval, both in the same and different regions, suggest that the denoising model generalizes to the noise from previous shots. These results demonstrate that the machine learning noise reduction method may contribute to reducing the data acquisition cost and time for marine seismic surveys in the future.

References

[1] Agata, R., Shiraishi, K., & Fujie, G. (2025). Physics-informed deep learning quantifies propagated uncertainty in seismic structure and hypocenter determination. Scientific Reports, 15(1), 1846.

[2] Durall, R., Ghanim, A., Fernandez, M. R., Ettrich, N., & Keuper, J. (2023). Deep diffusion models for seismic processing. Computers & Geosciences, 177, 105377.